Journal of Applied Fluid Mechanics, Vol. 17, No. 6, pp. 1217-1229, 2024.
Available online at www.jafmonline.net, ISSN 1735-3572, EISSN 1735-3645.
https://doi.org/10.47176/jafm.17.6.2419

Effect of Equivalence Ratio on Flame Morphology, Thermal and Emissions Characteristics of Inverse Diffusion Porous Burner

A. Dekhatawala, P. V. Bhale and R. Shah†

Department of Mechanical Engineering, Sardar Vallabhbhai National Institute of Technology, Surat, Gujarat, 395007, India

†*Corresponding Author Email: rds@med.svnit.ac.in*

ABSTRACT

The diffusion porous media combustion is one possible way to eliminate the drawbacks of the existing combustion systems. Inverse diffusion flame (IDF) has features of both premixed and non-premixed flames. To integrate the advantages of porous media combustion with IDF, inverse diffusion porous (IDP) medium burner is tested for change in flame morphology and emissions at different equivalence ratio (ϕ). The porous media located at the exit of IDF burner has potential to deliver minimum flame length with low emissions. Flame appearance, flame height, flame zones etc. and emissions are experimentally investigated. Methane is used as fuel. Visible flame height is captured digitally and evaluated using ImageJ software. Central plane flame temperature is measured experimentally. CO and NO_X emissions are recorded with Testo-340 flue gas analyser. The use of porous media at flame base is beneficiary in terms of achieving better air-fuel mixing and radial diffusion of air-fuel mixture. This reduces flame height with porous medium at all range of ϕ. Increase in ϕ reduces CO and enhances NO_X emissions. Porous media reduces CO by 75 % and NO_X by 60 %. Inverse diffusion porous medium burner emits lowest emissions in rich conditions.

Article History

Received November 7, 2023
Revised January 22, 2024
Accepted February 1, 2024
Available online March 27, 2024

Keywords:

Equivalence ratio
Flame morphology
Porous media burner
Inverse Diffusion combustion
CO and NO_X emissions

1. INTRODUCTION

The fast consumption of fossil fuel assets, lower efficiency and generation of higher pollutant emission from conventional combustion methodology encourages researchers to develop environmentally friendly and optimum fuel consuming combustion technology. The porous medium combustion (PMC) concept is seen as one of promising approach to meet these requirements. It can be easily adopted in many domestic and industrial applications.

The development of premixed PMC attracts many researchers due to advantages of higher thermal efficiency and lower emissions. Premixed porous medium burner can easily use as radiant burner and surface heaters (Sathe et al., 1990). For premixed PMC, the fundamental combustion stabilization principal is developed by Trimis and Durst (1996). The flame shape, speed, flame thickness and excess gas temperature of premixed air-methane combustion inside porous matrix is determined using two-dimensional non-equilibrium model by Sahraoui & Kavtany (1994). If the heat is used from hot gases of exhaust to preheat incoming reactants in combustion system, then the flame temperature of system is higher than the adiabatic flame temperature. This concept is known as excess enthalpy flames or superadibatic combustion and it is proposed by Weinberg, (1971). The superadiabatic combustion and subsequent combustion modes in porous structures is reported by Huang et al. (2002). Hayashi et al. (2004) had modelled three-dimensional two zone porous medium burner for numerical analysis of reacting flow. The numerical results of this study indicated that the steady flame front had seen at location of interference of two porous zones for wider operating range.

Kaplan and Hall (1995) reported experimental studies on PMC (magnesia-stabilized zirconia) using liquid fuel. They found that steady complete combustion and lowest emission of CO and NOx at range of equivalence ratio 0.57 – 0.67. Wu et al. (2012) attempted experimental investigation on pulse combustion of liquid fuel spray in porous media burner. It was suggested that the temperature of liquid combustion inside porous medium could controlled by varying the equivalence ratio. The changes in axial temperature of porous media burner at start up and switch off process experimentally evaluated by Wang et al. (2014). This study revealed that at higher flow rate or at small pellet diameter, to obtain

NOMENCLATURE

ϕ	equivalence ratio	NO_X	nitrogen oxides
Re_{air}	Reynolds number of air jet	*PMC*	porous medium combustion
V_r	velocity ratio	*LCM*	Low Concertation Methane
V_a	velocity of air jet	*LPG*	Liquified Petroleum Gas
V_f	velocity of fuel jet	*TPV*	Thermophotovoltaic
W^*	non -dimensional porous zone height	*PRTO*	Porous Implanted Regenerative Thermal Oxidizer
H^*	normalized flame height	ZrO_2	zirconium dioxide
z	axial distance	*VFD*	Variable Frequency Drive
r	radial distance	*SCADA*	Supervisory Control and Data Acquisition
IDF	Inverse Diffusion Flame	*SS*	Stainless Steel
IDP	Inverse Diffusion Porous	*LCV*	Lower Calorific Value
SiC	silicon carbide	*LPM*	Liter Per Minute
CO	Carbone monoxide	*PPI*	Pore Per Inch

superadibatic combustion mode in packed bed the critical equivalence ratio should be large. The divergent shape porous combustor has great potential compare to cylindrical shape combustor for better utilization of low concertation methane (LCM) due to variation of its concentration and flow rate (Lin et al., 2014). Laphirattanakul et al. (2016) experimentally investigated combustion stability of a self-entrained LPG porous burner at rich-premixed condition. They concluded that the convection mode of heat transfer and flame speed are main aspects governing flame stability in hollow cylindrical shape porous burner. Liu et al. (2019) experimentally and numerical investigated lean premixed propane-air combustion in porous burner. They observed that the flame shape was ellipsoid in porous zone. From experimentally investigation, Suo et al. (2022) presented combustion zone map to identify diversify of flame forms from lean to stoichiometry conditions.

PMC technology has also great potential to adopt for non-premixed mode of combustion applications such as IC engines (Durst & Weclas, 2001), gas turbine combustion (Jugjai & Pongsai, 2007) and thermophotovoltaic (TPV) power generation system (Qiu & Hayden, 2007). The fundamental mathematical model for diffusion flame in packed bed to determine flame height inside packed bed was developed and verified with experimental results by Kamiuto and Ogawa (2012). The flame stability of non- premixed PMC is higher at low equivalence ratio (Dobrego et al., 2001). The flame structure in plane parallel packed bed is starched out with rise of Reynold number and a ratio of the half breadth of burner to size of the packed sphere (Kamiuto & Miyamoto, 2004). The influence of swirl on the combustion efficiency and enhancement of radiation flux from porous burner was experimentally examined by Kamal and Mohamad (2005). They noted that the magnification in radiation flux was 5.7 times due to the optimum space between the swirling flow and inlet of porous zone. They also found that the emission level of CO and unburned hydrocarbon concertation was also reduced at higher swirling flow.

Zhang et al. (2013) developed porous implanted regenerative thermal oxidizer system (PRTO) using Zirconium dioxide (ZrO_2) ceramic foam for application in industrial copper melting furnace. The emission level of NO_x was significantly lower in PRTO. The fuel consumption of PRTO system was significantly reduced around 30% compare to conventional regenerative thermal oxidizer system. Ning et al. (2017) experimentally examined non-premixed methane/air combustion in Y shaped meso-scale combustion chamber. The Y shaped meso-scale combustion chamber was developed using fibrous porous media. They concluded that the flammability, stability and ignitability of methane-air diffusion flame can be boosted by using fibrous porous media. Endo Kokubun et al. (2017) carried out numerical analysis to scrutinize effect of mass injection rate and porosity on the extinction of a diffusion flame generated in porous medium. They identified the existence of a critical porosity beyond which a diffusion flame cannot be generated in porous zone, regardless the value of mass injection rate.

Peng et al. (2018) explored numerically non-premixed H_2/air combustion in cylindrical porous media combustor for application of micro-TPV system. From the numerical investigation it is found that increment of outer wall thickness or adding the porous medium enhance the heat transfer in micro combustor and influence the flame stability. Higher wall thickness and porous media give relatively higher uniform outer wall temperature. Shi et al. (2018, 2019) studied experimentally and numerically on diffusion filtration combustion in plane parallel packed bed with variation of height of packed bed and size of pellet. They observed that the variation in geometrical parameters of porous medium were strongly influencing flame structure, stability and emission level of CO and NO_x. The geometrical parameters of flame were affected by mass dispersion phenomena in porous zone. From the color variation of flame, it is proved that non-premixed mode of combustion was shifted to partially or fully premixed mode of combustion as the height of porous bed rise. They also observed that with increment of porous bed length and alumina pellet diameter, CO emission level increased while NO emission level decreased.

The above study exhibits that the majority research on PMC devoted towards the development of premixed mode of combustion. Only limited research is focused towards the development of non-premixed PMC. On the other hand, the non-premixed mode of combustion is widely accepted in many domestic and industrial applications due

to operational safety point of view. The major challenges of development of non-premixed PMC are efficient mixing of fuel and oxidizer inside porous medium as well as flame stability over wide range of oxidizer and fuel flow rates. IDF consists integral feature of premixed and non-premixed combustion.

IDF has features of both premixed and non-premixed flames. Optimum length and minimum emission requirements are driving force for the research in burner design. Physical mixing and chemical delay play decisive role in achieving these goals. Porous media located at the exit of IDF burner has potential to meet objectives of minimum flame length with low emissions. The objectives of the present study are to examine variation in flame morphology in terms of flame height, flame appearance, change in shapes and size of flame zones etc. and CO and NO_X emissions. Sensitivity of flame morphology and emissions are tested with respect to change in mixture strength, ϕ. The flame appearance of IDP burner is compared with and without porous medium cases. Visible flame height is captured and compared for variation in ϕ. Temperature on central vertical plane is measured experimentally and compared for porous and non-porous media cases. Nature and intensity of measured temperature distributions are associated to emissions characteristics of flames.

2. EXPERIMENTAL SETUP AND METHODOLOGY

Figure 1 shows the schematic diagram of the experimental setup for reactive experiments with IDP burner. The image of sophisticated experimental setup with essential instrument is also displayed in Fig. 2. The prime components of experimental set up of IDP burner are centrifugal blower (Fig. 2 (a)), air flow meter (Fig. 2(b)), fuel mass flow controller (Fig 2(c)) and control panel with variable frequency drive (VFD) (Fig 2 (e)). The thermal and emission characteristic of IDP burner during reactive testing are measured using B type (uncoated) thermocouple and flue gas analyzer (TESTO 340) (Fig. 2(d)) respectively. Centrifugal air blower supplies air through air flow line to air inlet of IDP burner. The speed of motor of centrifugal blower is controlled through VFD for variation in air flow rate. The air flow rate is measured using a calibrated thermal mass flow meter (LEOMI 586). This insertion type thermal mass flow meter metered volumetric air flow rate of air line with an accuracy of ± 2.0 % of the reading. The pure methane is supplied as gaseous form fuel in fuel line from pressurized cylinder. The fuel flow rate is controlled and measured by fuel mass flow controller (ALICATE MCR-50SLPM-D-D89). The measuring accuracy of fuel mass flow controller is ±0.8 % of the reading. Flame structure of IDP burner is observed through a glass window of enclosure which is provide on front side of enclosure. The images of flame shape and structure of IDP burner are captured using digital camera (SONY Alpha ILCE-6000Y). The supervisory control and data acquisition (SCADA) system is also integrated with centrifugal blower, VFD, air flow meter, fuel flow controller and thermocouple. This ensures precise control and record of various the thermal and flow parameters during reactive experiments. Table 1 indicates detail specifications of various measuring instruments.

The schematic of IDP burner with geometrical dimension is shown in Fig. 3(I). IDP burner is composed using square shape stainless steel (SS) pipes. To incorporate IDF conFiguration in IDP burner, air jet is introduced from central pipe. The inner diameter of central square pipe is 18 mm and a wall thickness of 1.2 mm. To make coaxial of burner, central pipe is surrounded by

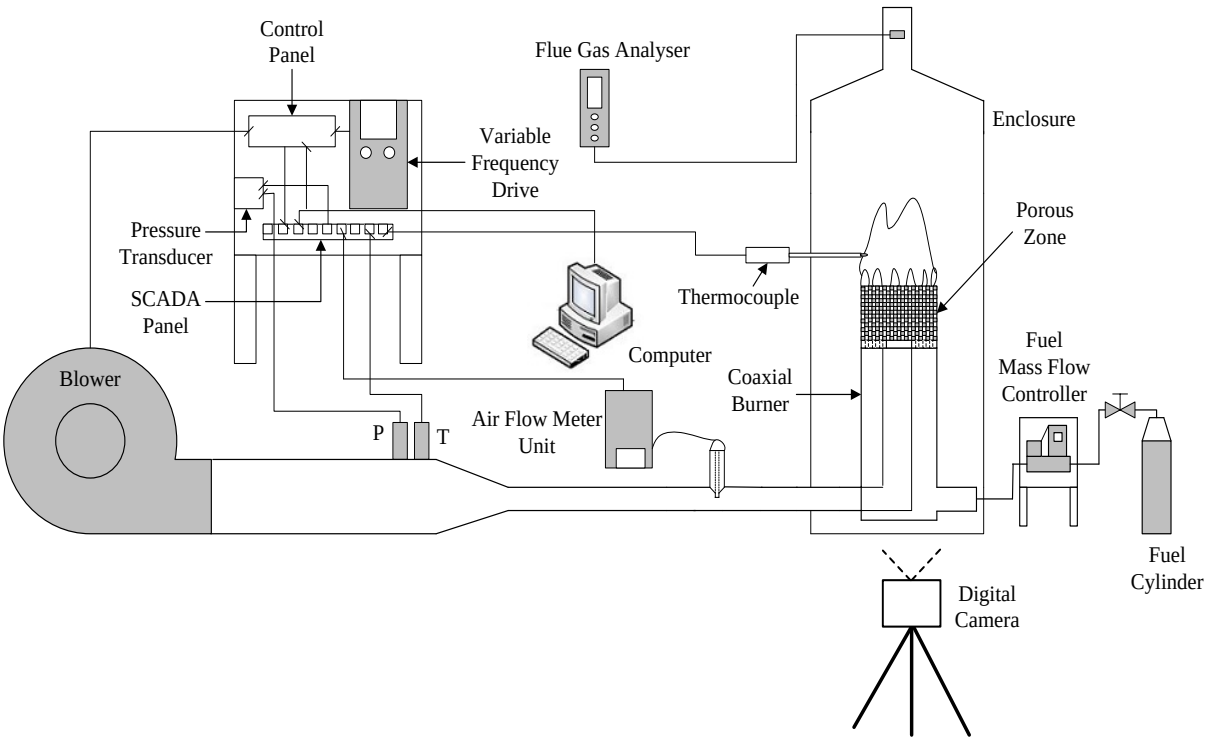

Fig. 1 Schematic diagram of experimental setup

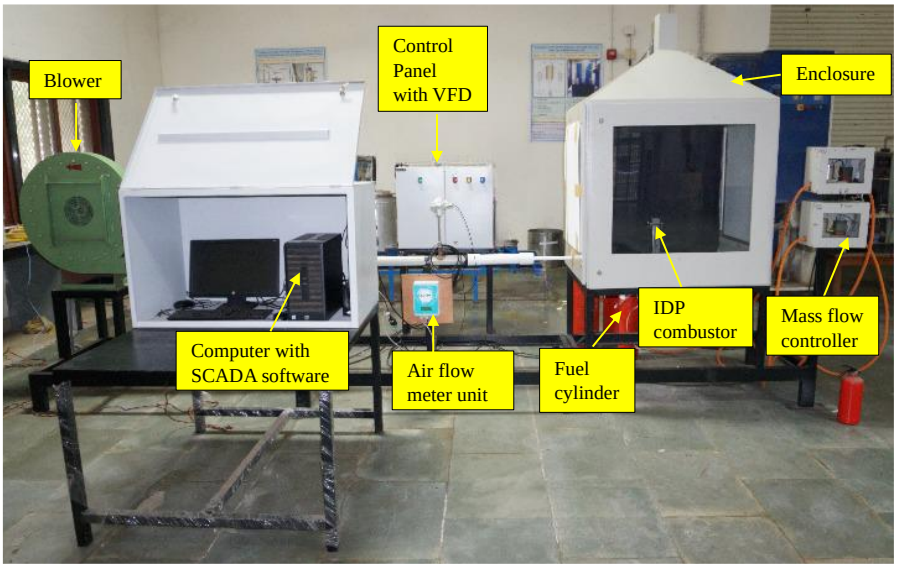

(a) Experimental setup

(b) Air flow meter

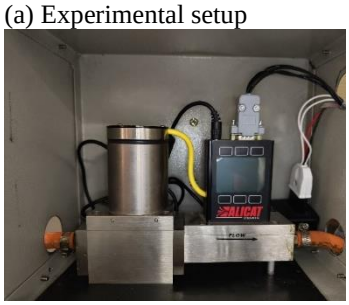

(c) Fuel mass flow controller

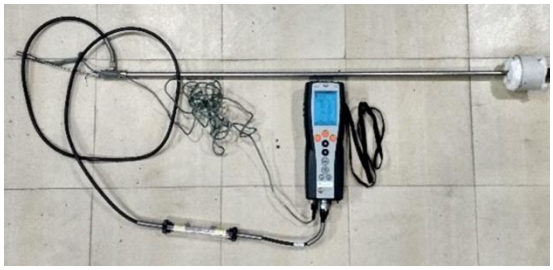

(d) Flue gas analyzer

(e) Control panel with VFD

Fig. 2 Image of experimental setup with major instruments

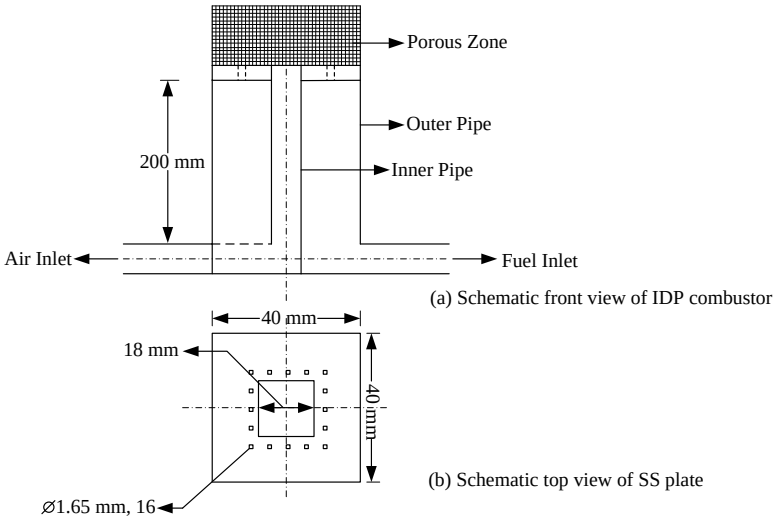

(a) Schematic front view of IDP combustor

(b) Schematic top view of SS plate

(I)

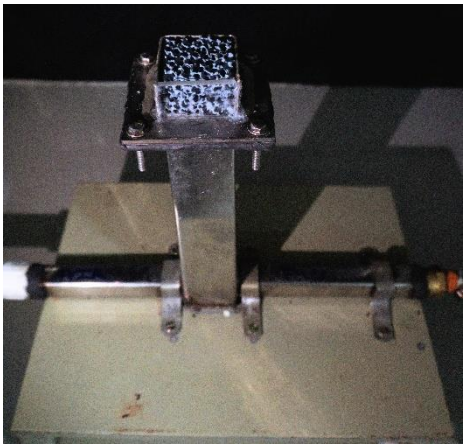

(II)

(III)

Fig. 3 (I) Schematic diagram of IDP burner, (II) Image of IDP burner , (III) Unstructured SiC ceramic porous block (10 PPI)

Table 1 Detail specifications of measuring instruments

Instruments	Range	Resolutions	Accuracy
Air flow meter	0 – 1000 LPM	0.01 LPM	±2.0%
Fuel mass flow controller	0 – 50 LPM	0.01 LPM	±0.8 %
Flue gas analyzer	0 - 500 ppm (Flue gas CO)	1 ppm (Flue gas CO)	±2 ppm (Flue gas CO)
	0 - 300 ppm (Flue gas NO_x)	1 ppm (Flue gas NO_x)	±2 ppm (Flue gas NO_x)
Type B Thermocouple	0 – 1700 ˚C	0.01˚C	± 2˚C

annular SS square pipe. The inner diameter of annular SS square pipe is 40 mm with a wall thickness of 1.2 mm. As per IDF conFiguration, fuel jet is discharged into porous zone of IDP burner through annular passage, which is created due to assembly of coaxial burner. To obtain adequate diffusion of fuel particles in to air in the porous zone, the fuel jet is divided into number of small jets. The detail design approach of division of fuel jet is reported in our previous work (Dekhatawala et al., 2023). Therefore, a square SS plate of 3 mm thickness with a central 18 mm square hole is fabricated. The diameter and number of fuel jets are described in schematic top view of SS plate (Fig. 3(I)). The casing of porous zone made from SS sheet with 2 mm thickness and the height of casing of the porous zone is 28 mm. A high temperature resistance glass is also fitted on the front side of casing of porous zone for observation whether the flame propagated inside porous zone or not. The final assembly of IDP burner is displayed in Fig. 3(II). The block of SiC ceramic foam (Fig. 3(III) is used as porous zone. The pore density and porosity of block of SiC ceramic foam are 10 PPI and 0.86 (Richardson et al., 2000) respectively.

In the present investigation, reactive experiments are conducted using pure methane as fuel. The impact of variation of ϕ ($0.6 \leq \phi \leq 1.4$) on flame morphology of IDP burner is studied considering fixed height of unstructured porous medium. The equivalence ratio is varied with increasing or decreasing the fuel flow rate, while air flow rate kept constant. The velocity of central air jet is represented in terms of non - dimensional Reynolds number (Re_{air}) which is determined from mass flow rate of air jet. The Re_{air} is calculated based on inner diameter of inner pipe and the other required fluid properties of air are considered at 30℃. As the fuel flow rate is varied, the supplied thermal energy of IDP burner is also altered which is determined considering lower calorific value (LCV) of methane. The detail experimental conditions are listed in Table 2.

3. RESULTS AND DISCUSSION

In present investigation, initial experiments are performed without porous zone with variation of ϕ. As the air flow rate is kept fixed at 143 LPM, only fuel flow rate is varied from 9.10 to 21.35 LPM, resulting in change in ϕ from 0.6 to 1.4. For same variation of ϕ and fixed height of porous medium reactive experiments are repeated. Table 2 describes investigated velocity ratio (V_r) and thermal energy input for respective ϕ. The height of porous zone, pore density and porosity are kept constant during experiments. The fixed height of porous zone is represented as non-dimensional height (W^*). W^* is obtained by dividing actual height of porous zone by inner diameter of annular pipe porous zone casing. The domination of ϕ on flame morphology of IDP burner without and with porous zone is scrutinized first. Then, impact of ϕ on flame height for both cases is analyzed, followed by emission aspect of IDP burner. Finally, central plane temperature contour of flame cone of IDP burner is compared with case without porous zone.

Table 2 Experimental conditions for constant air flow rate (143 LPM, Re_{air} = 8218)

Fuel flow rate (LPM)	ϕ	$V_r = V_a/V_f$	Energy input (KW)
21.35	1.40	0.90	11.73
19.81	1.30	0.97	10.88
18.30	1.20	1.05	10.05
16.73	1.10	1.15	9.19
15.21	1.00	1.26	8.35
13.80	0.90	1.39	7.58
12.15	0.80	1.58	6.67
10.66	0.70	1.80	5.86
9.10	0.60	2.11	4.99

3.1 Flame Appearance

Flame visualization and flame imaging are effective way to observe and understand influence of porous medium and air-fuel velocity ratio on flame morphology and luminosity. Figure 4 depicts flame morphology of an IDP burner. In IDF, flame base and flame torch connected via flame neck therefore it is called dual structure (Zhen et al., 2011). The pore distribution in porous zone of unstructured SiC ceramic block is random with varied pore size (Fig. 3(III)). Such structure of porous zone will provide flow resistance to air jet and fuel jets but prevents the propagation of flame inside porous medium. Thus, the unstructured SiC ceramic foam only acts as mixer medium. Flame in IDP burner consists single integral morphology in which flame base and torch can be recognized from the zone color as shown in Fig. 4.

Figure 5 compares the flame morphology of IDP burner at different ϕ without porous medium ($W^* = 0$). The velocity of air jet is fixed at the exit of burner and variation in ϕ is introduced by changing fuel flow rate. The flame appearance is slightly difference compare to pure IDF. In IDF, the ratio of air jet velocity to fuel jet velocity is high. Due to this higher ratio, fuel jet is entrained towards central air jet and intense combustion is initiated from the flame base (Patel & Shah, 2018). In IDP at $W^* = 0$, this ratio of velocities of air jet to fuel jet is in the range of 1 to 2 which is lower compare to pure IDF. So, the fuel jets are not much entrained toward air jet compare to pure IDF.

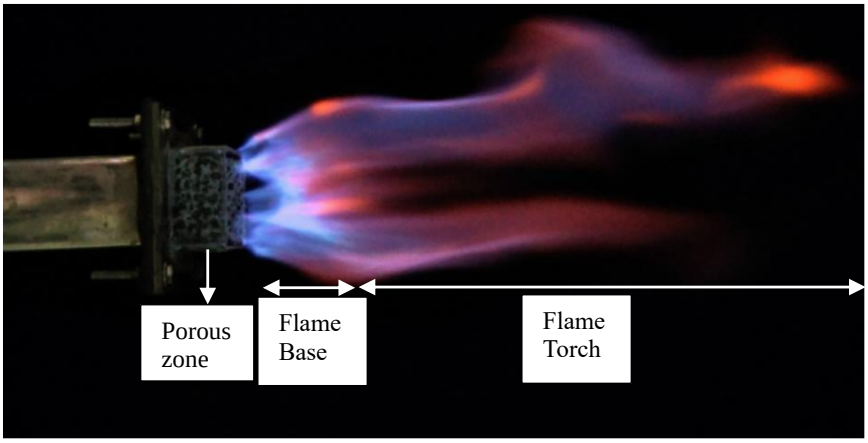

Fig. 4 IDP flame morphology

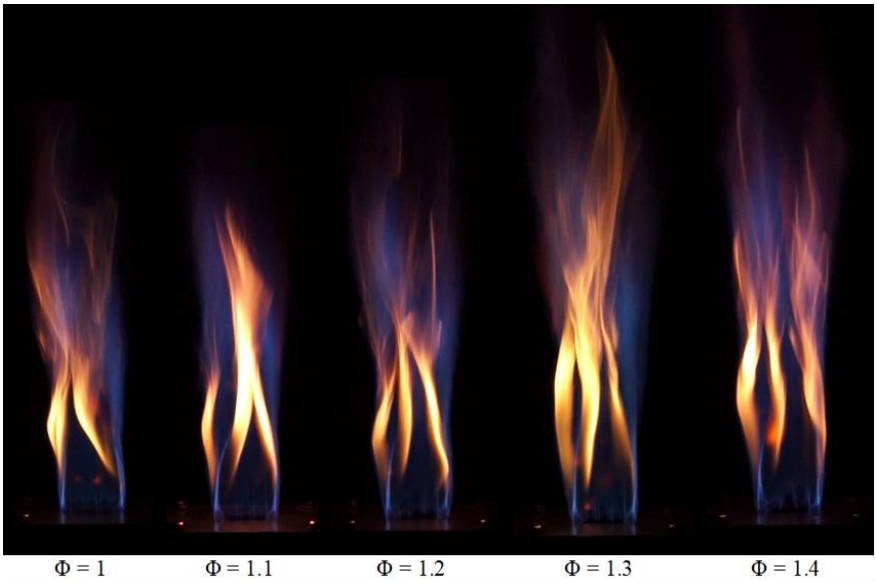

(a) (b) (c) (d) (e)

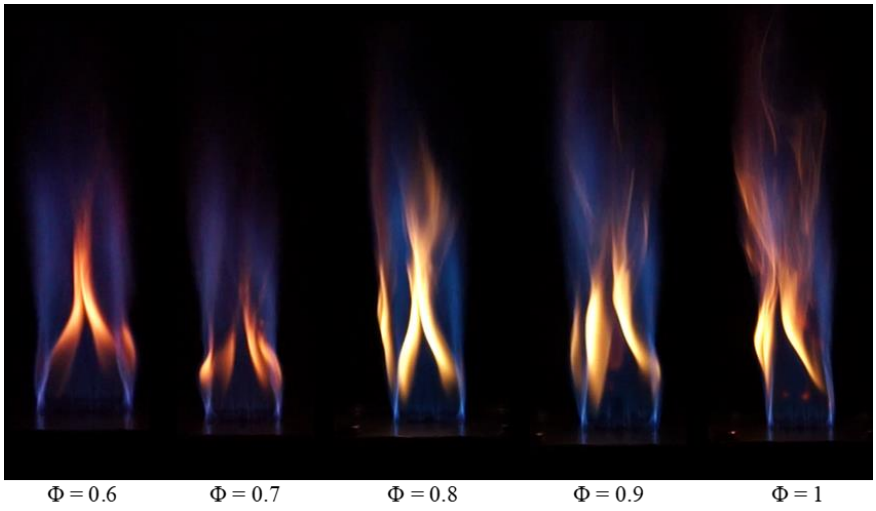

(f) (g) (h) (i) (j)

Fig. 5 Effect of ϕ on flame appearance of IDP burner at $W^* = 0$

The shape of flame base is not found inverted bowl shape and dark zone with thin blue zone at corners is appeared. This indicates the weak mixing of air and fuel jets at the flame base. The side and corners flame strips are overlapped each other's at downstream of flame torch. The color of flame torch is vigorous yellow- blue. From

the color of flame torch, it is observed that the diffusion mode of combustion with soot formation is predominated at flame torch region. At constant air flow rate, the variation in ϕ from1 to 1.4 is achieved by raising the fuel flow rate. This results in reduction of velocity ratio of air jet to fuel jet. This ultimately reduces the entrainment of fuel jet by central air jet. On the other hand, larger amount of fuel with higher velocity requires more time and length to mix with air. This leads to enhancement in overall extent of flame torch (Fig. 5 (a)-(e)). Opposite trend is observed when ϕ is lowered from 1 to 0.6 due to enhancement in velocity ratio and reduction in available amount fuel (Fig. 5 (f)-(j)). There is reduction in flame length as mixture becomes leaner. At low value of ϕ region of yellow flame reduces and region of blue flame increase. This indicates enhance fuel burning at lean conditions.

Figure 6 exhibits the influence of variation of ϕ on flame morphology with porous medium at W^* = 0.7, 10 PPI. The appearances of flame structure of IDP burner are inconsistent from previous case though the experimental flow conditions are same. The premixed zone (blue in color) and bright zone (orange – purple in color) are observed at flame base and flame torch respectively (Fig. 6). Due to presence of porous medium with W^* = 0.7, central air jet and fuel jets are spreading in radial direction inside the porous medium. Diffusion of fuel jets and air jet towards each other is happening in porous medium. This helps in premixing of fuel and air inside porous media in upstream of the flame base. In rich mixture strength situation (ϕ>1), fixed width flame is spotted. Porous media retards the flow and reduce the axial flow velocity. It imparts the radial velocity by forcing the fluid to pass through tiny pores distributed unevenly in all the directions. This improves physical mixing by having collision at molecular levels. Due to this intense blue zone is observed even in rich condition at flame base as shown in (Fig. 6(a)-6(e)). There are many flame holes are located inside the flame base. The flame hole is region in which burning of fuel is locally extinguished owing to higher strain rate imposed by the flow field on the reaction zone. In IDP burner at W^* =0.7, flame is emerged from number of tiny pores of SiC ceramic foam. In these tiny pores local

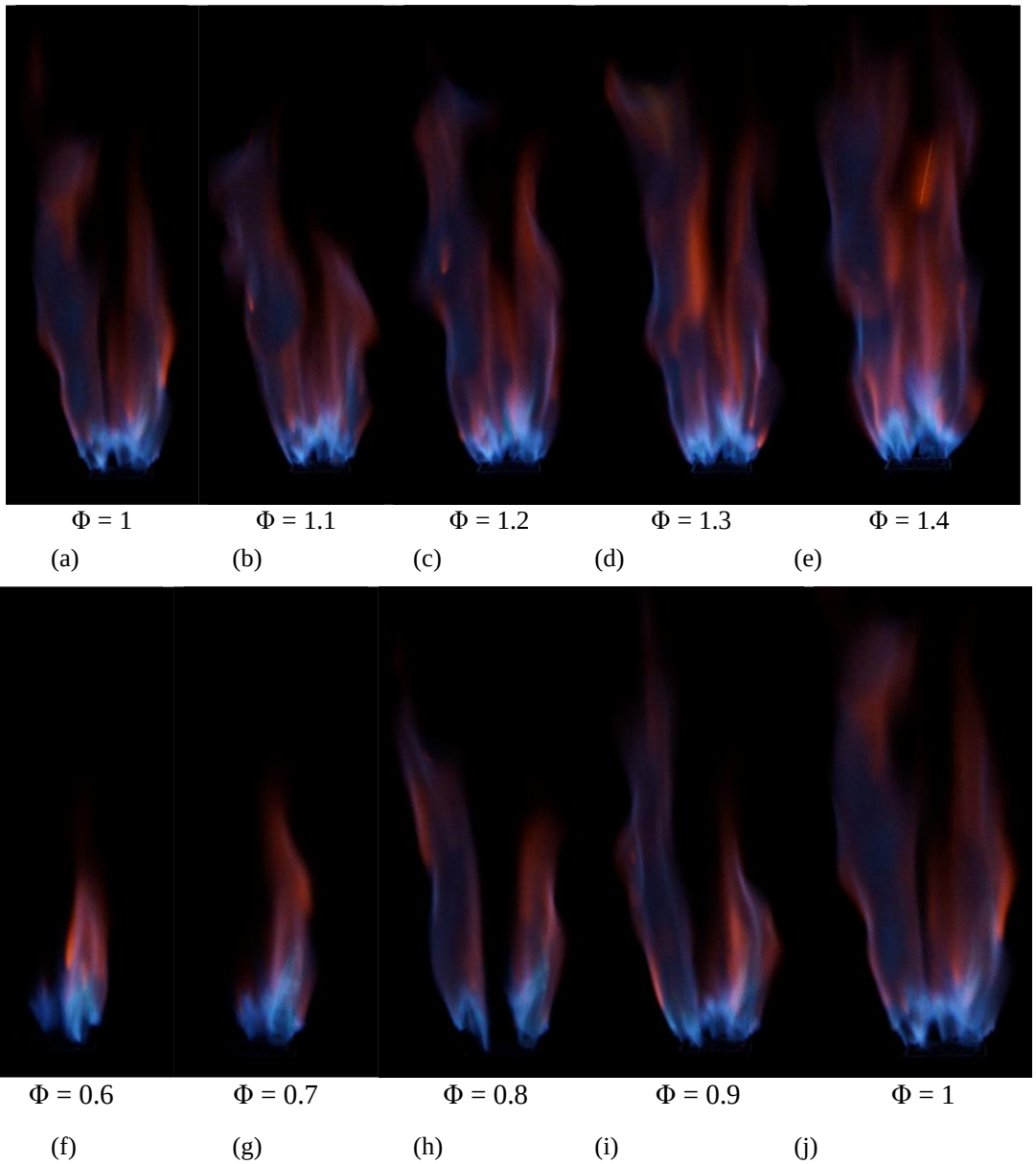

Fig. 6 Effect of ϕ on flame appearance of IDP burner at W^* = 0.7, 10 PPI

high-speed flow generates higher strain rate that cause flame to extinguish locally. The radial expansion and luminosity of flame torch reveals complete combustion of fuel occurred by utilizing the surrounding air. The flame structure is not stable at lean combustion conditions ($\phi<1$). At φ =0.9, the flame torch is divided in two distinct flame strip. Then the entire flame is bifurcated in two different flame strip (ϕ =0.8) and finally one flame strip is extinguished (ϕ =0.6). At lean condition value of velocity ratio (V_a/V_f) is in the range of 1.26 to 2.11. At lean condition, far away from stochiometric condition, the air velocity is almost twice that of fuel velocity. Low fuel velocity restricts the fuel entry in tiny pores and quality of physical mixing with air molecules. Due to this at lean operating conditions, the issue of flame stability is observed in IDP burner with W^* = 0.7.

3.2 Flame Height

Flame height is one of the essential performance features of IDP combustion that characterize the influence of porous medium on mixing quality of air and fuel jet inside the porous structure. The vertical distance from the exit of burner to visible flame tip is defined as flame height. In IDP combustion, porous medium is placed at top burner. So, in present scenario the height of porous medium is also added to estimate the flame height of IDP burner. The methodology to determine flame height from images of flame appearance is described elsewhere (Dekhatawala et al., 2023). The estimated flame height is normalized w.r.t. the inner diameter of air jet of the IDP burner. Figure 7 displays the plots of normalized flame height (H^*) of an IDP burner as a function of ϕ. It is observed that flame height rises with increment of ϕ for both cases. For case of W^* = 0, as ϕ rises, the velocity of fuel jet is also jump up with constant central air jet velocity which resulted in relatively poor fuel entrainment in air and remaining amount of fuel burned with surrounding air. The extension of reaction zone in axial direction is also identified from images of flame appearance of IDP burner (Fig. 5). Thus, flame height increases as ϕ rises.

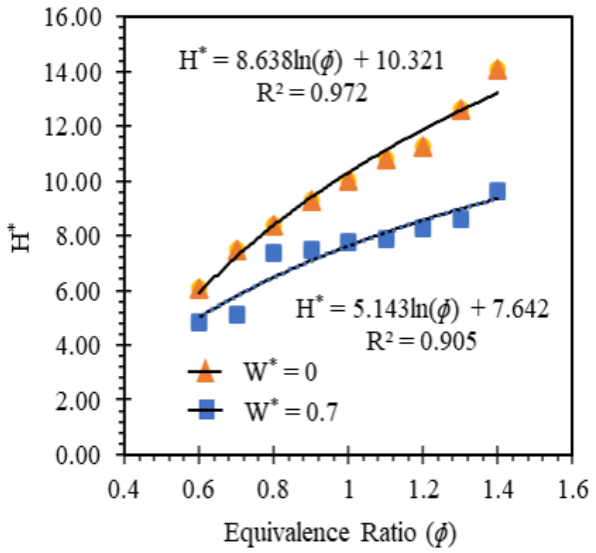

Fig. 7 Effect of ϕ on normalized flame height of IDP burner

In porous medium combustion, dispersion effect controls the visible flame height. For fixed height of porous zone, air jet and fuel jets are scattered inside the porous medium before combustion. Thus, the degree of mixing quality of combustible mixture is improved and intense combustion (blue zone) is found at flame base (Fig. 6). When ϕ is surged from 0.6 to 1.4 in case of W^* = 0.7, the dispersion effect in porous medium only enhances degree of mixing quality for combustible mixture without considerable alteration in residence time of mixture in porous media. Additional fuel at rich condition requires little more time to burn. This lead to rise in flame length with increment of ϕ in case of W^* = 0.7. From comparison of trend lines of both cases, there is sharp decrement in H^* from the range of 15 % to 29% for case of W^* = 0.7. At W^* = 0.7 and ϕ =1.4 flame height is comparable with W^* = 0 and ϕ=0.9. With porous media, at rich condition reduced flame height equivalent to lean conditions of without porous media can be obtained. The nature of variation for trend lines are logarithmic. The sharp fall in flame height with porous media indicate that the porous medium not only enhance combustion quality but it also minimized time required for mixing process before combustion in case of diffusion combustion. The experimental correlations of normalized flame height with equivalence ratio are also represented for both cases in Fig. 7. These are Valid for Re_{air} = 8218 in the range of ϕ from 0.6 to 1.4.

3.3 Central Plane Temperature Profile

In order to examine thermal characteristics of IDP flame, central plane temperature of flame cone is measured using type B (uncoated) thermocouple (bead diameter = 1mm, ± 2°C). The thermocouple is placed horizontal such that it remains perpendicular to flow of reactants. The measured temperature is corrected for radiation heat losses. (Brohez et al., 2004). In present burner geometry fuel jets are equally distributed around central fuel air jet (Fig 3 (I)). Thus, with respect to burner axis flame is symmetrical in vertical plane. Temperature profile is measured only in half plane starting from the burner axis.

Flame temperature is measured by thermocouple mounted on height gauge (size: 450 mm, least count: 0.02 mm). It is placed on cross sliding table. The entire assembly is shown in (Fig. 8). The thermocouple can be placed at required position by changing the position on height gauge (axial movement, z) and pointing sliding table at desired radial position, r, by rotating calibrated wheel of sliding table. Figure 9 exhibit various radial and axial locations for temperature measurement on central plane of flame. The radial position, r, at a fixed axial location is varied in the range of 0 to 30 mm with interval of 5 mm. The axial movement of thermocouple is considered within z= 5 mm to 75 mm with increment of 10 mm and z=75 to 125 mm with increment of 25 mm respectively.

Figure 10 shows measured temperature contours on central plane for W^* = 0 and W^* = 0.7. Figure 10 also compare experimentally measured temperature profiles of central plane with flame appearance images. The reactive

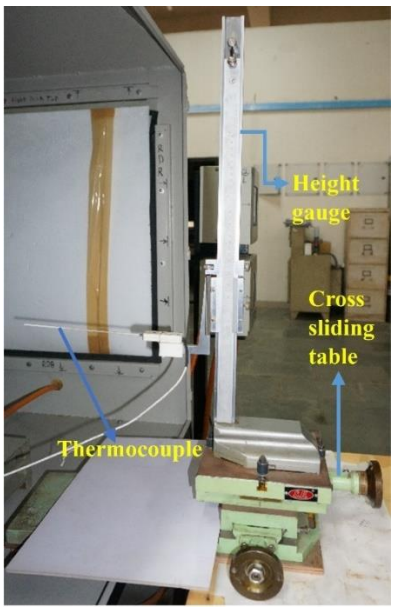

Fig. 8 Height gauge with cross sliding table assembly

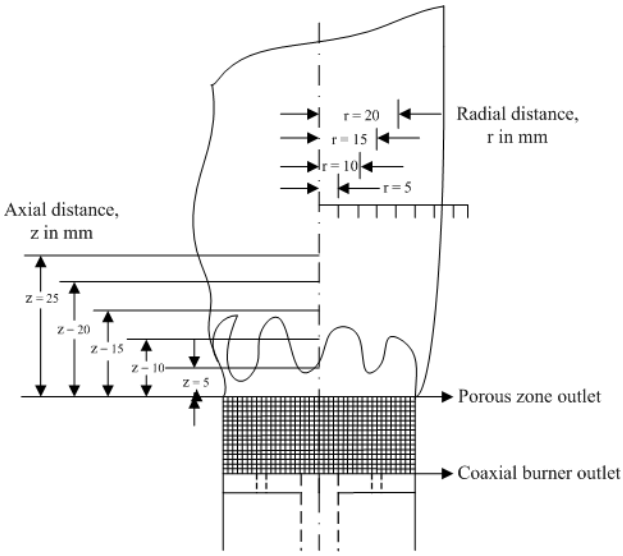

Fig. 9 Locations of temperature measurement

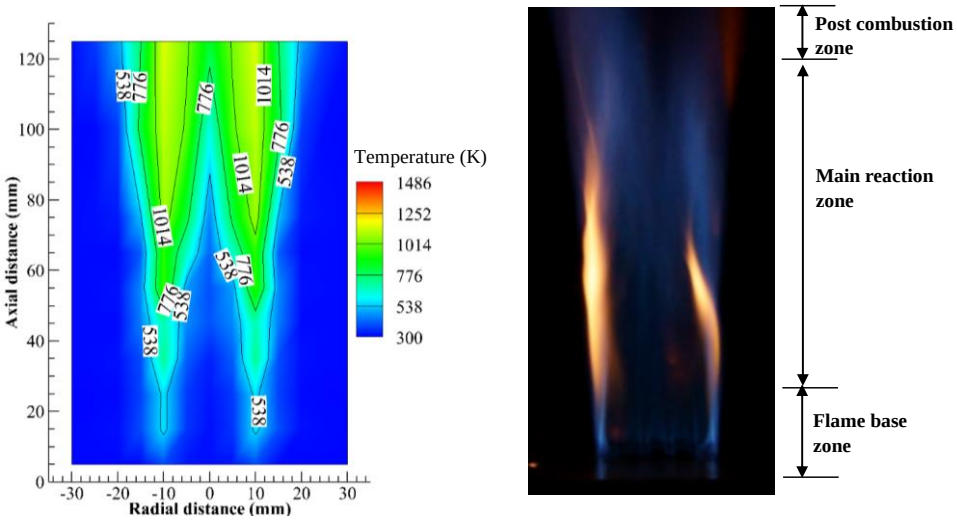

Experimental temperature profile **Flame apperance image**

(a) IDP burner at $W^* = 0$, $\phi = 1$

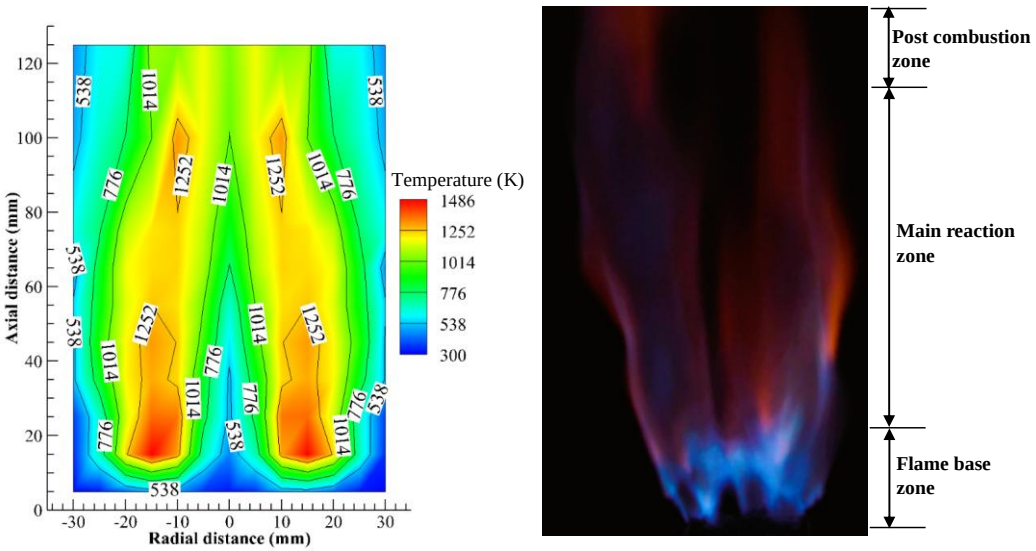

Experimental temperature profile **Flame apperance image**

(b) IDP burner at $W^* = 0.7$, $\phi = 1$

Fig. 10 Temperature profile (a) IDP burner at $W^* = 0$, $\phi = 1$ and (b) IDP burner at $W^* = 0.7$

zone of flame can be divided into three different characteristic zones. First zone is called flame base in which fuel and oxidizer are mixed with each other and combustion is initiated. Second zone is identified as main reaction zone in which is maximum heat is released due to the complete burning of fuel. Third zone is recognized as post combustion zone where cooling of hot combustion product occurs with entrainment of atmospheric air. For case $W^* = 0$ i.e., absence of porous zone, it is observed that the central area of flame base zone (z = 5 to 15 mm) is dark black and only two side corner flame strips are visible. The central dark black region in flame base zone signified. The dominance of central air jet and two side corner thin flame strips pointed out limited chemical reactions and associated heat released. The temperature of side corner flame strip is around 565 K. In main reaction zone (z = 15 to 75 mm), temperature is gradually rise up to almost two times of highest temperature of flame base. Additional entrainment of air also expanded the flame in radial direction at main reaction zone. This can also be verified from expansion of radial temperature profile (Fig. 10 (a)). The peak temperature (1154 K) is noted for case of $W^* = 0$ at z =125 mm which is post combustion zone. Thus, in IDP burner at $W^* = 0$, mixing process of air into fuel is extended from base zone to main reaction zone. The reaction rate and heat released rates are primary controlled by weak physical mixing. Mixing of air-fuel jets are having strong dependency on diffusion and entrainment. Mixing continue up to larger axial distance from burner base. This generates relatively larger flame length and subsequently maximum release of heat energy at post combustion zone.

Comparison of temperature contours for with and without porous case indicates that there is a major change in terms of flame shape, flame length and location of different flame zones. With porous media more uniform reactive flame surface is appearing compared to distinct flame strip of without porous case. Different distinct flame zones turned shorter and shifted to porous media. This results in shorter flame length compared without porous media case. The measured maximum flame temperature with porous media is around 1485 K at z=15 mm while the same without porous media is around 1154 K at z=125 mm. This change in IDP is due to diffusion and physical mixing of fuel and air jet inside the porous zone. Presence of porous zone at base of burner ensure uniform mixing of air and fuel. It also diffuses air and fuel radially. Presence of uniform blue zone at the flame base is due to diffusion and mixing phenomena happening in porous media. Porous media also conduct heat from reactive zone of flame to the fresh charge of air and fuel. This serves as pre heating of the charge before burning at flame surface (Mohamad, 2005). Preheating reduces chemical delay for mixture. Thus, as combined result of improved physical mixing and reduced chemical delay, the reaction rate is enhanced (Khaleghi et al., 2015). Over all accelerated fuel burning happens which produces high temperature and large heat near the flame base.

3.4 NO_x and CO Emission Characteristics

NO_x and CO emission characteristics of IDP burner with and without porous medium are measured at various values of ϕ. Testo 340 flue gas analyzer is used for emissions measurement. Figure 10 demonstrates effect ϕ on NO_x and CO emission characteristics of IDP burner. At $W^* = 0$, the CO emission is almost steady for all variation of ϕ (red line without fill square symbol in Fig. 11). For case of $W^*=0.7$, The CO emission rises linearly up to $\varphi=0.9$ then it is steady between $\phi = 0.9$ and $\phi = 1.1$. Further increment in ϕ beyond the 1.1, CO emission decreases (red line with fill square symbol in Fig. 11). Change in ϕ from 0.6 to 1.4 is brought by increasing fuel amount at constant air flow rate. Thus, the velocity ratio of air jet to fuel jet are reduced which ultimately reduced the entrainment of fuel particles in to central air jet. From images of flame appearance of $W^* = 0$ (Fig. 5), it is observed that some portion of blue regime of flame is expanded till flame tip. This blue regime specified that the availability of intermediate chemical species of CH^* and C_2^* at flame tip which are responsible for higher CO emission (Ikeda et al., 2002) in case of $W^*=0$. The influence of increasing ϕ on CO emission level is very limited in without porous medium case.

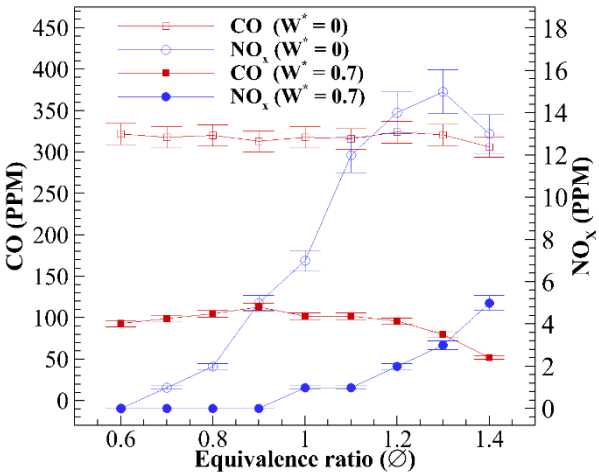

Fig. 11 Effect of ϕ on NO_x and CO emission

Porous media, $W^*=0.7$, reduces CO emission by three times compared to $W^*=0$. In case of $W^*=0.7$, fuel jets and air jets are mixed inside porous medium before combustion. Radial diffusion of air and fuel due to presence of porous medium not only increases level of physical mixing but also distributes combustible mixture in more part of radial plane near burner exit plane. Higher thermal conductivity of SiC ceramic compare to air also helps in conducting heat from reactive flame zone to porous medium in which air-fuel mixture is getting premixed. This results in pre heating of air-fuel mixtures. Pre heating reduces chemical delay and accelerate the combustion kinetics. Thus, with porous medium accelerated burning of fuel is achieved. The same can be observed by blue flame region near burner exit. Enhanced burning facilitates sufficient time for conversion of CO in to CO_2. Overall effect is low emission of CO with porous medium compared to without porous medium.

In combustion of hydrocarbon gases, the formation of NO_X contributed mainly by thermal NO_X, prompt NO_X and NO_X via N_2O intermediates. Percentage contribution

of NO_X via N_2O intermediates is very low compared to thermal and prompt mechanism at high temperature. Formation of thermal NO_X is controlled by Zeldovich mechanism. Rate of reactions involve in Zeldovich mechanism are temperature dependent such that higher NO_X is formed at high temperature (Hupa et al., 1989). Over all reactions of Zeldovich mechanism are slow thus prompt NO_X is generated only if residence time is long. Prompt NO_X formation is governed by Fenimore mechanism (Fenimore, 1971). Prompt NO_X is generated in fuel rich regions which are at relatively low temperature. In these regions efficiency of Zeldovich mechanism will be low.

Figure 11 describes dependency of NO_X on ϕ. NO_X emission without porous media is high compare to with porous media at same ϕ. For both cases NO_X increases with rise in ϕ. An increase in ϕ generally leads to more fuel in mixture with higher heat released. In case of without porous media, mixing of air and fuel takes place due to entrainment and diffusion. Thus, poor mixing of air and fuel results in reach region in the vicinity of flame surface. Due to this low luminous and low temperature flame as shown in Fig. 10(a) is generated in case of without porous media case. Low temperature flame and reach fuel region near flame triggers formation of prompt NO_X. When ϕ is surged from 0.6 to 1.4, the combustible mixture became lean to rich with increase rate of Fenimore reactions and produces higher prompt NO_X at more rich condition in case of without porous media. The large reduction in NO_X emission level is noted at $W^* = 0.7$ in contrast to $W^* = 0$ at same ϕ. At $W^* = 0.7$, in fuel lean conditions NO_X emission is almost nil. At fuel reach condition average reduction in NO_X is almost 6 times. In porous media air and fuel mix properly. This eliminates possibility rich fuel region at burner exit and there by reduces possibility of NO_X generation by prompt mechanism. Flame temperature with porous media is high (Fig. 10(b)) compared without porous media. The overall flame length is low in case of porous media. This low flame length reduces residence time for species. Low residence time offset the advantage of high temperature and thus suppress the formation of thermal NO_X. In case of $W^* = 0.7$, some amount heat is transferred through solid medium of porous zone to incoming fresh air-fuel mixture. This way, the required peak temperature, which is responsible to trigger the chain reactions of Zeldovich mechanism (Miao et al., 2016) is reduced which further suppress the NO_X emission levels. Li et al. (2019) also observed similar reduction in NO_X level with increment in height of packed bed in their experimental and numerical investigation.

4. CONCLUSION

Thermal and emission characteristics are measured experimentally for IDP burner. Variation of ϕ from lean to rich conditions is considered with and without unstructured porous medium using methane as a fuel. The prime observation based on present experimental study are listed below

1. Enhanced physical mixing of air with fuel and preheating of air-fuel mixture in porous media turns out in accelerated combustion near flame base region.
2. The visible flame height, CO and NOx emission level of IDP burner are declined almost 25%, 75% and 60% respectively for case of IDP burner with $W^* = 0.7$ compare to $W^* = 0$ in all variation of ϕ.
3. The peak flame temperature on central plane near exit of porous medium is elevated by 28.6% for $W^* = 0.7$ and $\phi = 1$.
4. In the range of $\phi = 1.2$ to 1.4, the IDP burner with $W^* = 0.7$ outperforms in terms of low flame height and less emissions.
5. The utilization of porous media under fuel reach condition is recommended for high-speed combustion system where burning time of fuel is limited as well as high rate of energy release is required.

CONFLICT OF INTEREST

The authors have no competing interests or conflicts to disclose.

AUTHORS CONTRIBUTION

A. Dekhtawala established lab setup and conducted experiments, drafted the manuscript, and arranged all plots. **R. Shah** supervised and guided the work. Finally, **P. V. Bhale** reviewed, edited and finalised the manuscript before submission.

REFERENCES

Brohez, S., Delvosalle, C., & Marlair, G. (2004). A two-thermocouples probe for radiation corrections of measured temperatures in compartment fires. *Fire Safety Journal*, *39*(5), 399-411. https://doi.org/10.1016/j.firesaf.2004.03.002

Dekhatawala, A., Bhale, P. V., & Shah, R. (2023). Experimental investigation on effect of height and pore density of porous medium on flame and emission characteristics of inverse diffusion combustor. *Thermal Engineering*, (In press).

Dobrego, K. V., Kozlov, I. M., Zhdanok, S. A., & Gnesdilov, N. N. (2001). Modeling of diffusion filtration combustion radiative burner. *International Journal of Heat and Mass Transfer*, *44*(17), 3265–3272. https://doi.org/10.1016/S0017-9310(00)00343-4

Durst, F., & Weclas, M. (2001). A new type of internal combustion engine based on the porous-medium combustion technique. *Proceedings of the Institution of Mechanical Engineers, Part D: Journal of Automobile Engineering*, *215*(1), 63–81. https://doi.org/10.1243/0954407011525467

Endo Kokubun, M. A., Fachini, F. F., & Matalon, M. (2017). Stabilization and extinction of diffusion

flames in an inert porous medium. *Proceedings of the Combustion Institute*, *36*(1), 1485–1493. https://doi.org/10.1016/j.proci.2016.07.004

Fenimore, C. P. (1971). *Formation of nitric oxide in premixed hydrocarbon flames.* Symposium (International) On Combustion, Elsevier. https://doi.org/10.1016/S0082-0784(71)80040-1

Hayashi, T. C., Malico, I., & Pereira, J. C. F. (2004). Three-dimensional modelling of a two-layer porous burner for household applications. *Computers and Structures*, *82*(17–19), 1543–1550. https://doi.org/10.1016/j.compstruc.2004.03.050

Huang, Y., Chao, C. Y. H., & Cheng, P. (2002). Effects of preheating and operation conditions on combustion in a porous medium. *International Journal of Heat and Mass Transfer*, *45*, 4315–4324. https://doi.org/10.1016/S0017-9310(02)00137-0

Hupa, M., Backman, R., & Boström, S. (1989). Nitrogen oxide emissions of boilers in Finland. *JAPCA*, *39*(11), 1496-1501. https://doi.org/10.1080/08940630.1989.10466644

Ikeda, Y., Kojima, J., & Hashimoto, H. (2002). Local chemiluminescence spectra measurements in a high-pressure laminar methane/air premixed flame. *Proceedings of the Combustion Institute*, *29*(2), 1495-1501. https://doi.org/10.1016/S1540-7489(02)80183-3

Jugjai, S., & Pongsai, C. (2007). Liquid fuels-fired porous burner. *Combustion Science and Technology*, *179*(9), 1823–1840. https://doi.org/10.1080/00102200701260179

Kamal, M. M., & Mohamad, A. A. (2005). Enhanced radiation output from foam burners operating with a nonpremixed flame. *Combustion and Flame*, *140*(3), 233–248. https://doi.org/10.1016/J.COMBUSTFLAME.2004.12.001

Kamiuto, K., & Miyamoto, S. (2004). Diffusion flames in plane-parallel packed beds. *International Journal of Heat and Mass Transfer*, *47*(21), 4593–4599. https://doi.org/10.1016/J.IJHEATMASSTRANSFER.2003.08.032

Kamiuto, K., & Ogawa, T. (2012). Diffusion flames in cylindrical packed beds. *Journal of Thermophysics and Heat Transfer*, *11*(4), 585–587. https://doi.org/10.2514/2.6284

Kaplan, M., & Hall, M. J. (1995). The combustion of liquid fuels within a porous media radiant burner. *Experimental Thermal and Fluid Science*, *11*(1), 13–20. https://doi.org/10.1016/0894-1777(94)00106-I

Khaleghi, M., Hosseini, S. E., Wahid, M. A., & Mohammed, H. A. (2015). The effects of air preheating and fuel/air inlet diameter on the characteristics of vortex flame. *Journal of Energy*, 2015. https://doi.org/10.1155/2015/397219

Laphirattanakul, P., Laphirattanakul, A., & Charoensuk, J. (2016). Effect of self-entrainment and porous geometry on stability of premixed LPG porous burner. *Applied Thermal Engineering*, *103*, 583–591. https://doi.org/10.1016/j.applthermaleng.2016.03.079

Li, H., Shi, J., Mao, M., & Liu, Y. (2019). Experimental and numerical studies on combustion characteristics of N_2-diluted CH_4 and O_2 diffusion combustion in a packed bed. *Royal Society open science*, *6*(9), 190492. https://doi.org/10.1098/rsos.190492

Lin, B., Dai, H., Wang, C., Li, Q., Wang, K., & Zheng, Y. (2014). Combustion characteristics of low concentration coal mine methane in divergent porous media burner. *International Journal of Mining Science and Technology*, *24*(5), 671–676. https://doi.org/10.1016/j.ijmst.2014.03.027

Liu, H., Wu, D., Xie, M., Liu, H., & Xu, Z. (2019). Experimental and numerical study on the lean premixed filtration combustion of propane/air in porous medium. *Applied Thermal Engineering*, *150*, 445–455. https://doi.org/10.1016/j.applthermaleng.2018.12.155

Miao, J., Leung, C. W., Cheung, C. S., Huang, Z. H., & Zhen, H. S. (2016). Effect of hydrogen addition on overall pollutant emissions of inverse diffusion flame. *Energy*, *104*, 284-294. https://doi.org/10.1016/j.energy.2016.03.114

Mohamad, A. A. (2005). *Combustion in porous media: fundamentals and applications*. Transport phenomena in porous media III (pp. 287-304). Pergamon. https://doi.org/10.1016/B978-008044490-1/50015-6

Ning, D., Liu, Y., Xiang, Y., & Fan, A. (2017). Experimental investigation on non-premixed methane/air combustion in Y-shaped meso-scale combustors with/without fibrous porous media. *Energy Conversion and Management*, *138*, 22–29. https://doi.org/10.1016/j.enconman.2017.01.065

Patel, V., & Shah, R. (2018). Experimental investigation on flame appearance and emission characteristics of LPG inverse diffusion flame with swirl. *Applied Thermal Engineering*, *137*, 377-385. https://doi.org/10.1016/j.applthermaleng.2018.03.105

Peng, Q., Jiaqiang, E., Chen, J., Zuo, W., Zhao, X., & Zhang, Z. (2018). Investigation on the effects of wall thickness and porous media on the thermal performance of a non-premixed hydrogen fueled cylindrical micro combustor. *Energy Conversion and Management*, *155*, 276–286. https://doi.org/10.1016/j.enconman.2017.10.095

Qiu, K., & Hayden, A. C. S. (2007). Thermophotovoltaic power generation systems using natural gas-fired radiant burners. *Solar Energy Materials and Solar*

Cells, *91*(7), 588–596. https://doi.org/10.1016/j.solmat.2006.11.011

Richardson, J. T., Peng, Y., & Remue, D. (2000). Properties of ceramic foam catalyst supports: pressure drop. *Applied Catalysis A: General*, *204*(1), 19-32. https://doi.org/10.1016/S0926-860X(00)00508-1

Sahraoui, M., & Kavtany, M. (1994). Direct simulation vs volume-averaged treatment of adiabatic, premixed flame in a porous medium. *International Journal of Heat and Mass Transfer*, *37*(18), 2817-2834. https://doi.org/10.1016/0017-9310(94)90338-7

Sathe, S. B., Peck, R. E., & Tong, T. W. (1990). A numerical analysis of heat transfer and combustion in porous radiant burners. *International Journal of Heat and Mass Transfer*, *33*(6), 1331–1338. https://doi.org/10.1016/0017-9310(90)90262-S

Shi, J., Liu, Y., Liu, Y., Mao, M., Xia, Y., Ma, R., & Xu, Y. (2018). An experimental study on coflow diffusion combustion in a pellet-packed bed with different bed lengths. *Royal Society Open Science*, *5*(8). https://doi.org/10.1098/rsos.172027

Shi, J., Liu, Y., Mao, M., Lv, J., Wang, Y., & He, F. (2019). Experimental and numerical studies on the effect of packed bed length on CO and NOx emissions in a plane-parallel porous combustor. *Energy*, *181*, 250–263. https://doi.org/10.1016/j.energy.2019.05.141

Suo, S., Shen, Z., Shi, J., Chen, Z., Zhang, Y., Jiang, L., Zhang, Y., Qi, H., & Xie, M. (2022). Wake flow and flame characteristics in the porous media with different surface combustion states: An experimental study. *Chemical Engineering Science*, *257*, 117677. https://doi.org/10.1016/J.CES.2022.117677

Trimis, D., & Durst, F. (1996). Combustion in a porous medium-advances and applications. *Combustion Science and Technology*, *121*(1–6), 153–168. https://doi.org/10.1080/00102209608935592

Wang, H., Wei, C., Zhao, P., & Ye, T. (2014). Experimental study on temperature variation in a porous inert media burner for premixed methane air combustion. *Energy*, *72*, 195–200. https://doi.org/10.1016/j.energy.2014.05.024

Weinberg, F. J. (1971). Combustion temperatures: The future? *Nature*, *233*(5317), 239–241. https://doi.org/10.1038/233239a0

Wu, D., Liu, H., Xie, M., Liu, H., & Sun, W. (2012). Experimental investigation on low velocity filtration combustion in porous packed bed using gaseous and liquid fuels. *Experimental Thermal and Fluid Science*, *36*, 169–177. https://doi.org/10.1016/j.expthermflusci.2011.09.011

Zhang, J. C., Cheng, L. M., Zheng, C. H., Luo, Z. Y., & Ni, M. J. (2013). Development of non-premixed porous inserted regenerative thermal oxidizer. *Journal of Zhejiang University: Science A*, *14*(9), 671–678. https://doi.org/10.1631/JZUS.A1300198/FIGURES/8

Zhen, H. S., Choy, Y. S., Leung, C. W., & Cheung, C. S. (2011). Effects of nozzle length on flame and emission behaviors of multi-fuel-jet inverse diffusion flame burner. *Applied Energy*, *88*(9), 2917-2924. https://doi.org/10.1016/j.apenergy.2011.02.040